Changes in Cerebral Connectivity and Brain Tissue Pulsations with the Antidepressant Response to an Equimolar Mixture of Oxygen and Nitrous Oxide: an MRI and Ultrasound study

Thomas Desmidt (t.desmidt@chu-tours.fr)
University Hospital of Tours
Paul-Armand Dujardin
Frédéric Andersson
Inserm
Bruno Brizard
UMR 1253, iBrain, Université de Tours, Inserm, France https://orcid.org/0000-0002-0110-822X
Jean-Pierre Remeniéras
Valérie Gissot
https://orcid.org/0000-0002-0091-8159
Nicolas Arlicot
https://orcid.org/0000-0001-7087-2312
Laurent Barantin
UMR INSERM U1253 iBrain https://orcid.org/0000-0002-5119-658X
Fabien Espitalier
Catherine Belzung
INSERM 1253 and University of Tours https://orcid.org/0000-0001-6095-5974
Arnaud Tanti
INSERM https://orcid.org/0000-0003-4249-2317
gabriel robert
rennes 1 university https://orcid.org/0000-0003-2490-0700
Samuel Bulteau
Quentin Gallet
François Kazour
Sandrine Cognet
Vincent Camus
https://orcid.org/0000-0002-6845-221X
Wissam El-Hage
Pierre Poupin
Helmet Karim

https://orcid.org/0000-0002-9286-0694

Article

Keywords: nitrous oxide, treatment resistant depression, functional connectivity, anterior cingulate cortex, brain tissue pulsatility

Posted Date: March 2nd, 2023

DOI: https://doi.org/10.21203/rs.3.rs-2612390/v1

Abstract

Nitrous oxide (N_2O) has recently emerged as a potential fast-acting antidepressant but the cerebral mechanisms involved in this effect remain speculative. We hypothesized that the antidepressant response to an Equimolar Mixture of Oxygen and Nitrous Oxide (EMONO) would be associated with changes in cerebral connectivity and brain tissue pulsations (BTP).

Thirty participants (20 depressed and 10 healthy controls - HC) were exposed to a one-hour single session of EMONO and followed for one week. Cerebral connectivity of the Anterior Cingulate Cortex (ACC, seed based resting state blood oxygen level dependent) and BTP (as assessed with ultrasound Tissue Pulsatility Imaging) were compared before and after exposure (as well as during exposure for BTP) among HC, non-responders and responders. Response was defined as a reduction of at least 50% in the MADRS score one week after exposure.

Nine (45%) depressed participants were considered responders and eleven (55%) non-responders. In responders, we observed a significant reduction in the connectivity of the subgenual ACC with the precuneus. Connectivity of the supracallosal ACC with the mid-cingulate also significantly decreased after exposure in HC and in non-responders. BTP significantly increased in the 3 groups between baseline and gas exposure, but the increase in BTP within the first ten minutes was only significant in responders.

We found that a single session of EMONO can rapidly modify the functional connectivity in the ACC, especially in the subgenual region, which appears to contribute to the antidepressant response. In addition, larger increases in BTP, associated with a significant rise in cerebral blood flow, appear to promote the antidepressant response, possibly by facilitating optimal drug delivery to the brain. Our study identified potential cerebral mechanisms related to the antidepressant response of N_2O, as well as potential markers for treatment response with this fast-acting antidepressant.

1. Introduction

Nitrous oxide (N_2O) has recently emerged as a potential fast-acting antidepressant, based on a series of randomized controlled trials that showed a rapid action of N_2O to reduce depressive symptoms in patients with treatment-resistant depression (TRD) [1–5]. The therapeutic procedure generally involved patients with TRD, exposed to one or more sessions of one-hour gas exposure, constituted most of the time by a mixture of $50\%O_2/50\%N_2O$ (also labelled as Equimolar Mixture of Oxygen and Nitrous Oxide – EMONO), which is the most commonly used packaging for medical use such as analgesia. Responders to the gas generally exhibit a symptomatic improvement within two hours, an effect that tends to last at least one week, although exact duration of response remains unknown and has not been systematically investigated to date.

The antidepressant effects of N_2O is thought to involve glutamatergic cerebral pathways, similar to ketamine, another fast-acting antidepressant, although N_2O induces only partial blockage of NMDA

receptors as opposed to the full NMDA blockage observed with ketamine [6]. Additionally, preclinical studies found that mice exposed to N_2O showed increased synaptic glutamate-mediated transmission, similar to ketamine [7]. N_2O has also been found to promote hippocampal neurogenesis in rats, which may also contribute to its antidepressant effect [8]. However, to date, the cerebral mechanisms involved in the antidepressant effects of N_2O in patients with depression remain largely speculative.

Cerebral connectivity, assessed with resting-state functional MRI, can be used to investigate functional impairments in the brain of patients with psychiatric disorders, including depression that has been associated with functional connectivity changes that could be restored with successful treatment [9]. Among the connectivity maps, the anterior cingulate cortex (which is constituted of subgenual, perigenual and supracallosal - or dorsal - regions, respectively labelled as sgACC, pgACC and scACC) has been suggested to constitute a major hub where impairments in this network may contribute to depressive symptoms [10]. More specifically, depression has been associated with elevated baseline levels of activity in sgACC, whereas normalization of this over-activity is thought to be an important biomarker of a successful antidepressant treatment [10].

Other correlates of antidepressant response include changes in Brain Tissue Pulsations (BTP) as assessed with the recently developed ultrasound neuroimaging methods of Tissue Pulsatility Imaging (TPI). Indeed, findings from our group identified excessive brain pulsatile movements in patients with depression [11], which are restored to safer level in responders to conventional antidepressants [12]. This ultrasound technique has the advantage to be easily implemented in various protocols such that changes in BTP can be easily investigated during gas exposure.

The goal of our study was to investigate pre- and post-treatment changes (as well as per-treatment for BTP) in cerebral connectivity and BTP among healthy controls (HC) and depressed participants (identified as responders or non-responders to the gas) exposed to a single one-hour EMONO exposure. We hypothesized that the antidepressant response to EMONO would be associated with reduction in the ACC connectivity and in BTP. We chose to focus on the ACC because of the previous evidence related to the contribution of ACC in depression as well as preliminary findings that identified strong changes in ACC connectivity in a single depressed patient exposed to N_2O [13]. We also chose to investigate BTP during the procedure because N_2O has been associated with large increases in cerebral blood flow (CBF) [14] which is major determinant of BTP and could facilitate optimal drug delivery to the brain.

2. Methods

2.1 Participants

Twenty participants with a major depressive episode (MDE) and 10 heathy controls (HC) were recruited from our in- and outpatients psychiatric care units or from the clinical investigation center records, respectively. We chose to include only females with a limited age range (25–50 years old) in order to limit the variability of brain reactivity related to age and sex, and the possibility of group differences since

responders and non-responders are determined *a posteriori*. Participants in the depressed group had to meet DSM-IV criteria for MDE with a severity score > 20 on the Montgomery–Asberg Depression Rating Scale (MADRS) and were resistant to at least one well conducted antidepressant, as assessed with the MGH-ATRQ. Non-inclusion criteria included bipolar or schizophrenic disorder, neurocognitive disorders, substance abuse disorder, counter-indication to MRI, pregnancy and legal guardianship. Counter-indications to EMONO exposure (intracranial hypertension, vigilance impairment, severe head trauma, pneumothorax, emphysema, abdominal gas distension, recent use of ophthalmic gas - SF6, C3F8, C2F6, known and untreated deficit in vitamin B12 or B9, recent unexplained neurologic impairments), the presence of active and significant psychotic symptoms, as well as any unstable somatic disease that could interfere with EMONO diffusion (neurological, cardiac or lung diseases) were also non-inclusion criteria. HC had no psychiatric and no significant medical condition, and a MADRS score lower than 5. Exclusion criteria included a positive pregnancy test, a deficit in vitamin B12 and clinically significant abnormalities in MRI. The study was approved by the French National Agency (MEDAECPP-2019-07-00014) and an independent national research ethics committee (17.07.04.43355). The project was registered on the ClinicalTrials.gov website (NCT04199143) and was supervised by a clinical investigation center (Inserm CIC1415). All of the patients signed informed-consent forms before enrolling in the trial.

2.2 Study design

The study design was a 1-week open-labeled EMONO trial with 4 visits, at baseline, Day 0 (day of exposure), Day 1 and Day 7. All the visits occurred in the clinical investigation center of the university hospital of Tours, France. After informed consent, the baseline visit consisted in clinical and psychometric assessments, vitamin B12 dosage and a first MRI scan. The second visit (Day 0) generally occurred two days after the baseline visit, with a maximum of 5 days between visits, depending on the availability of the MRI scan, and consisted in the EMONO exposure and ultrasound assessments followed by the second MRI scan and psychometric assessment, two hours after exposure. A second dosage of vitamin B12, ultrasound measures and clinical and psychometric assessments were performed on Day 1 (the day after EMONO exposure). The final visit on Day 7 (one week after EMONO exposure) consisted in clinical and psychometric assessments.

2.3 Clinical and psychometric assessments

The clinical assessment included blood pressure, height and weight measurements. Psychometric assessments were performed by a senior psychiatrist (TD) and included clinician-rated questionnaires (the MADRS for the severity of the depressive symptoms, the Clinical Global Impressions (CGI) for a general assessment of the disease severity, the Scale for Suicidal Ideations (SSI) for the severity of suicidal symptoms and risk, the Young Mania Rating Scale (YMRS), the Clinician Administered Dissociative States Scale (CADSS) and the Brief Psychiatric Rating Scale (BPRS) for the potential presence and severity of, respectively, manic, dissociative and delusional symptoms) and self-rated questionnaires namely the Quick Inventory of Depressive Symptomatology Self Report (QIDS-SR), the State-Trait Anxiety Inventory (STAI), the Visual Analogical Assessment (VAS) for the severity of,

respectively, depressive symptoms, anxiety symptoms and a general assessment of the participant's well-being. All these measures were performed at baseline, Day 0 (two hours after exposure), Day 1 and Day 7, in the depressed participants only (except the MADRS that was performed at baseline for the HC). The MADRS was used to classify participants regarding their response status. Depressed participants with a MADRS reduction of 50% or greater at Day 7 compared to baseline were considered responders, otherwise non-responders.

2.5 EMONO exposure

Gas exposure was performed using EMONO bottles marketed as KALINOX® (Air Liquide, France), which include 4.4m^3 of a 50%N_2O/50%O_2 mixture, a pressure regulator and an integrated flow meter of 15 liters. We use this conditioning of EMONO because this is how N_2O is the most commonly used in medical settings, for instance as an analgesic to reduce pain during potentially painful examinations. We referred to the method for N_2O exposure described in [4]. All the participants were exposed to a one-hour EMONO exposure accordingly. The whole procedure was performed in the clinical investigation center by a trained nurse, under the supervision of a senior medical doctor (VG). EMONO was delivered via high concentration facial masks to limit gas loss. Masks were connected to a specific monitor to continuously measure N_2O concentration. Gas flow was generally between 9 and 12L/min, a parameter that was adjusted by the nurse during the procedure in order to reach the targeted 50% N_2O concentration that tend to decrease because masks are not fully airtight. Total N_2O delivery was calculated for each participant as follows: gas flow (L/min) x time of exposure (Min) (Table 1).

Table 1
Comparisons of the clinical and ultrasound characteristics among responders, non-responders and healthy controls. Values are expressed as the median (interquartile range) or n (%). Comparisons were performed with Kruskal-Wallis or Mann-Whitney tests (quantitative data) and chi-squared tests (qualitative data).

	Responders (n = 9)	*Non-responders (n = 11)*	*Healthy Controls (n = 10)*	*p value*
Age (years)	39.0 (15.0)	37.0 (9.0)	34.5 (15.0)	0.973
BMI (kg/m^2)	23.1 (7.5)	24.8 (10.2)	23.6 (12.7)	0.707
SBP (mmHg)	122.0 (11.0)	120.0 (27.5)	119.5 (22.3)	0.979
DBP (mmHg)	79.0 (4.0)	76.0 (15.5)	77.0 (16.0)	0.992
Number of previous MDE	1.0 (2.0)	3.0 (1.5)	-	0.459
Duration of MDE (weeks)	32.0 (74.0)	52.0 (94.0)	-	0.675
Current medications, antidepressants				
SSRI	5 (55.5%)	4 (36.4%)	-	0.391
SNRI	4 (44.4%)	7 (63.6%)	-	0.391
TeCA	2 (22.2%)	2 (18.2%)	-	0.822
Current medications, others				
Benzodiazepine	2 (22.2%)	4 (36.4%)	-	0.492
Lamotrigine	0	3 (27.3)	-	0.089
Quetiapine	1 (11.1%)	0	-	0.257
Valpromide	1 (11.1%)	0	-	0.257
MADRS Baseline	28.0 (5.0)	31.0 (4.0)	-	0.285
MADRS Day 7	9.0 (6.0)	26.0 (13.0)	-	10^{-4}
CGI Baseline	5.0 (1.0)	5.0 (0.5)	-	0.249
CGI Day 7	2.0 (2.0)	4.5 (1.5)	-	10^{-4}
SSI Baseline	1.0 (8.5)	1.0 (4.0)	-	0.725
SSI Day 7	0.0 (0.0)	0.0 (4.0)	-	0.178
QUIDS-SR Baseline	20.0 (4.0)	18 (5.0)	-	0.789
QUIDS-SR Day 7	8.0 (6.0)	15.5 (16.0)	-	0.022

	Responders (n = 9)	*Non-responders (n = 11)*	*Healthy Controls (n = 10)*	*p value*
STAI Baseline	47.0 (23.5)	55.0 (21.0)	-	0.323
STAI Day 7	39.0 (12.5)	60.0 (16.75)	-	0.013
VAS Baseline	40.0 (5.0)	50.0 (26.0)	-	0.700
VAS Day 7	70.0 (12.5)	50.0 (35.0)	-	0.017
Duration of EMONO exposure (min)	60.0 (19.0)	60.0 (5.0)	60.0 (7.5)	0.587
Quantity of N_2O delivered (Liter)	507.0 (390.0)	540.0 (99.0)	540.0 (234.8)	0.710
Vitamine B12 Baseline	249.0 (55.5)	247.0 (153.0)	290.5 (151.0)	0.548
Vitamine B12 Day 1	276.0 (60.5)	256.0 (157.0)	291.0 (186.2)	0.659
MeanBTP Baseline (µm)	8.3 (4.1)	5.7 (4.7)	5.0 (1.7)	0.211
MeanBTP Day 1 (µm)	6.2 (6.9)	7.8 (8.9)	5.0 (5.1)	0.961
MaxBTP Baseline (µm)	53.9 (34.5)	33.5 (17.6)	39.45 (15.3)	0.255
MaxBTP Day 1 (µm)	23.0 (41.0)	47.7 (37.3)	34.3 (16.5)	0.583

BMI: Body Mass Index; SBP: Systolic Blood Pressure; DBP: Diastolic Blood Pressure; MDE: Major Depressive Episode; SSRI: Selective Serotonin Reuptake Inhibitor ; SNRI: Serotonin-Norepinephrine Reuptake Inhibitor ; TeCAs: TertraCyclic Antidepressant ; MADRS: Montgomery Asberg Depression Rating Scale; QIDS-SR: Quick Inventory of Depressive Symptomatology Self-Report ; CGI: Clinical Global Impression ; SSI : Scale for Suicide Ideation ; STAI-Y-A: State-Trait Anxiety Inventory ; VAS : Visual Analogue Scale; BTP: Brain Tissue Pulsations ; EMONO : Equimolar Mixture of Oxygen and Nitrous Oxide

Participants were continuously monitored for vitals (oximetry, blood pressure, heart and respiratory rates). Additional safety monitoring included behavioral disorders and neurologic deficits, especially vigilance disorders. After the exposure, all the participants received 15 minutes of 100% O_2 to limit the risk of hypoxia and were monitored for at least 2 hours after the exposure. Finally, they were assessed one last time by the medical doctor before they were authorized to safely leave the facility.

2.5 MRI Protocol

MR scans were collected at our hospital setting using a 3T Siemens PRISMA using a Siemens 20-channel head coil. A sagittal, whole brain T1-weighted magnetization prepared rapid gradient echo (MPRAGE) was collected with repetition time (TR) = 2300 ms, echo time (TE) = 2.98 ms, flip angle (FA) = 9 deg, field of view (FOV) = 256x256, 1 mm^3 isotropic resolution, no gap, and no acceleration. An axial, whole-brain fluid attenuated inversion recovery (FLAIR) sequence was collected to appropriately identify white/gray

matter as well as WMH, a marker of cSVD. This sequence had TR = 8260 ms, TE = 130 ms, FA = 150 deg, FOV = 186x230, 0.9 x 0.9 x 2.5mm resolution, 2.5 mm gap, and no acceleration. We collected an axial, whole brain echo-planar imaging (EPI) sequence to measure blood-oxygen dependent responses during resting state. This sequence had a TR = 1850 ms, TE = 30 ms, FA = 34 deg, FOV = 192x192, 3 x 3 x 3.7 mm resolution, 3.68mm gap, and no acceleration. A gradient echo field map was also collected for correction with TR = 660 ms, TE = 4.7 ms and 7.82 ms, FA = 25 deg, FOV = 280x280, 2.2 x 2.2 x 3 mm resolution, and 3mm gap. Overall, scanning lasted approximately 30 minutes and included other scans, which are not the focus of the current manuscript.

We conducted structural and functional preprocessing of MRI using SPM12 unless otherwise noted [15]. All interpolations were done using 4th degree B-spline while similarity metrics were mutual information (for motion correction) or normalized mutual information (coregistration between different image types). FLAIR was coregistered to the MPRAGE then jointly segmented using unified segmentation to output 6 tissue classes. Number of Gaussians for white matter were set to two to account for white matter hyperintensities. Segmentation outputs a deformation field used to normalize fMRI to a standard anatomical space (Montreal Neurological Institute, MNI, space). We created an automated intracranial mask by combining threshold maps of gray matter, white matter, and CSF (probability of 0.1) then conducting image filling and image closing, which was used to skull strip the MPRAGE.

Resting state data was slice-time corrected, motion corrected, skull stripped with BET (brain extraction tool in FSL), coregistered to the skull-stripped MPRAGE (using mean fMRI as reference), normalize to MNI space (using previous deformation field), and spatially smoothed (full-width at half-maximum of 8mm). We then conducted wavelet despiking using BrainWavelet Toolbox, which uses data-driven and a locally-adaptive denoising method to deal with motion spike artefacts [16]. We regressed out the following using SPM: 6 parameters of motion from motion correction, 5 eigenvariates of white matter and CSF (i.e., CompCor) [17], and sinusoids corresponding to unwanted frequencies outside of the band-pass in resting state (i.e., a band-pass filter 0.008–0.15 Hz). This was done as to not reintroduce artefact or noise back into our signal [18].

We computed functional connectivity maps for the anterior cingulate (ACC) using the AAL3 atlas [19] for the left and right subgenual (sgACC), pregenual (pgACC), and supracallosal (scACC). We computed the eigenvariate in each region and computed whole-brain Pearson correlation maps, which we transformed into Z-scores by subtracting the global and dividing by the standard deviation.

2.6 Ultrasound Protocol

Ultrasound assessments were performed at Day 0 before, during and after EMONO exposure, as well as at Day 1, by a trained investigator (PAD or BB) who was blinded for the clinical response. Ultrasound assessments consisted in measuring Brain Tissue Pulsations (BTP) according to the Tissue Pulsatility Imaging (TPI) technique which was previously used in experimental tasks involving HC and clinical populations, including participants with depression [11, 12, 20, 21]. BTP measures were performed on an ArtUS ultrasound scanner (Telemed; Lithuania). Transcranial acquisitions were performed with a P5-

1S15-A6 phased-array transducer (Telemed; Lithuania). Measurements were performed through the right temporal bone window with the probe firmly maintained by a mechanical holder to reduce artifacts caused by the subject's movements. Color Doppler was used to center the US beam on the right Middle Cerebral Artery (MCA). The US scanner was then switched to Echo-B mode to perform BTP measurements centered on the MCA. With this configuration, we explored the circle of Willis and a transversal slice of the temporal hemispheres.

For each subject, the whole protocol consisted of 2 minutes acquisitions, realized at different times: 12 acquisitions the day of exposure (one just before exposure, at H + 2min, H + 4min, H + 6min, H + 8min, H + 10min, H + 18min, H + 28min, H + 38min, H + 48min, H + 58min and one after exposure), and one acquisition the day after EMONO administration. However, some participants were agitated after 10 minutes of exposure which resulted in noisy signal and only 6 per-treatment acquisitions were kept for the final analysis. The US scanner provided direct access to beam-formed radiofrequency (RF) lines, which were used to estimate BTP. The data were then downloaded for offline analysis with MATLAB® software (MathWorks Inc., USA).

Our method described in the following lines assesses the z axis component of brain displacements. The z axis is perpendicular to the US probe surface and the x axis is long the probe surface. The ultrasound (US) firing sequence includes of a group of M broad-view focused pulsing events that are transmitted in order. Between adjacent firings, the transmission (TX) steering angle θ (i.e., the propagation angle with respect to the transducer surface normal) is incrementally changed so as to cover a span of M angles over the entire group of pulsing events. For each focused transmission TX at a particular θ angle, beamformed IQ data line is obtained from echoes acquired from the transducers. At each time instant t, we estimate the brain tissue motion independently at all the pixel positions. For a particular pixel of interest situated on a US line referenced by the transmit angle θ, we used the temporal lag-one autocorrelation algorithm [22] to estimate the phase shift $\Delta\varphi$between successive complex IQ data. We used the revised form [23] of the Doppler equation

$$\Delta\Phi = \frac{2\pi T}{\lambda}\left(\overrightarrow{V}.\overrightarrow{n}_{TX} + \overrightarrow{V}.\overrightarrow{n}_{RX}\right)$$

1

used for vector flow estimation, where $\overrightarrow{V}$ is the Doppler tissue velocity, λ the US wavelength, T the IQ temporal discretization interval, $\overrightarrow{n}_{TX}$ the direction of the ultrasound (US) propagation in transmit mode TX, and $\overrightarrow{n}_{RX}$ the direction of the US RX beamforming [22]. In our application, these two vectors directions are identical and $\overrightarrow{n}_{TX} = \overrightarrow{n}_{RX} = \overrightarrow{n}$ with $\overrightarrow{n} = (sin\theta, cos\theta)$. Thus, the phase shift $\Delta\Phi$ estimated by our algorithm expressed

$$\Delta\Phi = \frac{4\pi T}{\lambda}\overrightarrow{V}.\overrightarrow{n} = \frac{4\pi T}{\lambda}(V_x sin\theta + V_z cos\theta)$$

2

.

This Doppler phase shift $\Delta\Phi$ is angle θ dependent and is also impacted by the lateral tissue velocity V_x. In our application, the blood flow induces a swelling of the brain which creates mainly a radial displacement. Since the US probe is situated perpendicularly to the skull, then quasi perpendicularly to the external brain surface, the V_x tissue velocity component oriented along the x axis in (2) is weak and we will neglect it in this work. Then, the Doppler phase shift expression can be simplified to $\Delta\Phi = \frac{4\pi T}{\lambda} V_z cos\theta$ which allows us to determine the component V_z of the brain tissue velocity along the depth axis from

$$V_z = \frac{\lambda}{4\pi T} \frac{1}{cos\theta} \Delta\Phi$$

3

Z axis displacement u_z is obtained from the cumulative summation of V_z in the temporal domain.

We obtained a 3D matrix of BTP: axial displacements u_z (x, z, t) along the z axis, x axis and time t. We analyzed the temporal evolution of BTP at each position of the 2D plane. As previously described, we used two criteria to filter out artifacts and focus on physiological signals [11, 12, 20, 21]. The first criterion consisted in the ratio of the second maximum peak over the central peak (SMP/CP) of the temporal autocorrelation function of each kernel. If the ratio SMP/CP was higher than 0.6, the record was validated and confronted to the second criterion. The cumulated standard deviation (CSTD) of the pulsations was calculated to inform on the data dispersion and was normalized to the peak-to-peak amplitude (Umean) of the mean temporal curve. If the ratio CSTD/Umean was lower than 0.25, the record was validated, otherwise rejected. The thresholds for the 2 criterion were based on previous studies [11, 24].

From this final matrix, we calculated the root mean square of 2 curves, MaxBTP and MeanBTP, corresponding, respectively, to the curve with the maximum of the mean peak-to-peak amplitude (averaged between cycles) and to the averaging of all curves in the matrix. MaxBTP and MeanBTP thus correspond to the pulsatility of, respectively, the greater and the mean pulsatility in the whole region of acquisition.

2.7 Statistical Analyses

After been visually checked using histogram, BTP measures were not considered normally distributed so we performed non-parametric analyses to investigate differences in BTP among groups at baseline and Day 1 (kruskal wallis' tests) and longitudinal changes within groups (pre-, per- and post-treatment using Friedman's tests).

We performed voxel-wise statistical analyses with statistical non-parametric mapping (SnPM12) [25]. This approach computes non-parametric p-values using permutation testing (10,000 permutations) while

thresholding with a cluster-forming threshold of p = 0.001. We then controlled the family wise error rate (FWE) at α = 0.05. For the left and right subgenual (sgACC), pregenual (pgACC), and supracallosal (scACC) connectivity maps we conducted several voxel-wise analyses. To test for differences from pre- to post-treatment, we conducted a paired t-test between pre- and post-treatment connectivity in controls, responders, and non-responders. To test for group differences at pre-treatment, we conducted a 1-way ANOVA (comparing the three groups) with the pre-treatment connectivity. To test for group differences at post-treatment, we conducted a 1-way ANOVA (comparing the three groups) with the post-treatment connectivity. To test for interaction effects between time and group, we computed a difference map between pre- and post-treatment connectivity and then conducted a 1-way ANOVA between groups on the difference map. These analyses test for time, group, and group x time effects voxel-wise for each map.

3. Results

3.1 Efficacy of EMONO exposure

Nine (45%) depressed participants were considered responders, whereas eleven (55%) were considered non-responders, based on a reduction of at least 50% at the MADRS on Day 7. There was no significant difference in clinical and baseline depression characteristics among the groups (responders versus non-responders and HC when applicable), as shown in Table 1. Symptoms of depression (and related symptomatology) showed no significant difference at baseline, whereas all the symptomatic measures (clinician- and self-rated) were significantly lower in responders compared to non-responders at Day 7, except for SSI, which scores were low in the two groups. There was no difference among groups in duration of exposure and quantity of N_2O delivered (Table 1). The full psychometric assessments performed at each of the 4 visits are shown in Supplementary Materials 1.

3.2 Tolerability of EMONO exposure

For 17 (57%) participants, gas exposure was considered well-tolerated with no particular side effect. The two main side effects were vomiting (n = 7, 23%) and agitation (n = 6, 20%). One participant also experienced deep sedation and desaturation that rapidly improved when we stopped the procedure and administered 100% oxygen for few minutes. Finally, we observed no significant increase in manic, dissociative or delusional symptoms (Supplementary Materials 1).

3.3 Functional connectivity

We found that significant decrease in right sgACC to precuneus connectivity in responders (x = 6, y=-64, z = 46, T_{max}=7.0, 127 voxels, see Fig. 1). We also found a time x group effect for right scACC to mid cingulate connectivity (x=-6, y = 18, z = 30, F_{max}=29.4, 208 voxels, see Fig. 1). We conducted *post-hoc* tests for differences. Pairwise comparisons showed that sgACC-precuneus connectivity was significantly lower after treatment only in responders ($t(8) = 6.520$, $p < 10^{-4}$). Supracallosal ACC-mid cingulate connectivity was significantly greater at baseline in HC compared to responders ($t(17) = 3.248$, $p = 0.005$) and non-responders ($t(19) = 3.628$, $p = 0.002$). Pairwise comparisons showed that dorsal ACC connectivity

was significantly lower after treatment in HC ($t(9) = 6.778$, $p < 10^{-4}$) and significantly greater after treatment in non-responders ($t(9)=-3.289$, $p = 0.009$).

3.4 Ultrasound Brain Tissue Pulsations

There was no significant difference among groups in Mean and MaxBTP at baseline (pre-treatment) or at Day 1 (post-treatment) (Table 1). We found no significant change in Mean or Max BTP between baseline and Day 1 in any of the three groups. MeanBTP values during exposure were all significantly greater compared to baseline values in all the 3 groups ($p < 0.05$, for all pairwise comparisons between the baseline value and the 5 per exposure values, in each of the 3 groups), suggesting a rapid and significant increase in BTP with EMONO (Fig. 2). When comparing BTP values within the 10 first minutes of exposure, we found a significant increase in MeanBTP in responders ($\chi^2_2 = 15.438$, $p = 0.004$, with pairwise differences between MeanBTP at 2 minutes and 6 minutes, $p = 0.001$, 8 minutes, $p = 0.004$, and 10 minutes, $p = 0.003$) but not in non-responders ($\chi^2_2 = 5.534$, $p = 0.237$) or HC ($\chi^2_2 = 2.800$, $p = 0.592$). We observed no significant differences with MaxBTP.

4. Discussion

We found that a single one-hour exposure to EMONO can rapidly modify the functional connectivity in the brain and significantly increase the amplitude of brain pulsations, notably in individuals with depression who respond to the gas. More specifically, the antidepressant response was associated with a reduction in the connectivity of the sgACC with the precuneus that has been considered a critical hub for depression pathophysiology [26]. Elevated baseline levels of activity in sgACC are observed in depression and normalization of this hyperactivity is thought to be an important biomarker of successful antidepressant treatment [10]. Interestingly, reduction in the BOLD signal of the sgACC was found to be the most rapid and sustained neuronal change associated with ketamine, another fast-acting glutamatergic antidepressant [10]. More broadly, cerebral mechanisms associated with the antidepressant effect of ketamine has been related to shutting off the affective network, for which the sgACC is a central hub. More specifically, lowering the connectivity between the sgACC and the precuneus may participate to block ruminations and improve the phenomenology of depression [27]. Finally, our results suggest that EMONO, similar to ketamine, can rapidly reduce the connectivity between the sgACC and the precuneus, which appears to be a key mechanism for the rapid antidepressant action.

Our results suggest a second cerebral mechanism that may participate to the antidepressant effect of EMONO, as shown with the significant elevation of BTP during the first ten minutes of exposure. BTP can be assessed with the ultrasound technique of TPI that has a high level of detection to measure micro-movements and very subtle brain pulsations that may be related to changes in CBF in our study. Indeed, N_2O is well known to induce large arterial vasodilation and large increases in CBF [14], which is a major determinant of BTP [28, 29]. While we observed a plateau in the BTP increase with EMONO in controls and non-responders (after a very large immediate BTP elevation in all the participants), global brain pulsations, as assessed with meanBTP, continued to increase in responders during the first ten minutes of

exposure, an effect that may have participated to the antidepressant action of the gas, although we cannot be sure that the increase in BTP was superior for these patients compared to the other groups. A possible explanation is that a large increase in CBF facilitates optimal drug delivery to the brain, not only because the quantity of active principles may be greater but also because the blood brain barrier shows broad opening with a continuous rise in CBF [30, 31] which facilitates N_2O to cross from the arteries to the specific neuronal targets, possibly glutamatergic neurons for the antidepressant effect. Finally, elevation in BTP may participate to the antidepressant effect of N_2O as well as provide a biomarker for treatment response, such that the larger the increase the better response. However, this remains to be confirmed in larger studies with larger sample size.

We found that the connectivity in the dorsal (or supracallosal) ACC with the middle cingulate, which was greater at baseline in controls compared to the depressed groups, decreased in controls after EMONO exposure whereas it increased in non-responders and showed no significant changes in responders. Because there was no change in the connectivity of the dorsal ACC in responders, we can assume that this effect is not related to the antidepressant effect of EMONO. Rather, it may be involved in the analgesic effect of the gas since it is a well-documented therapeutic action of EMONO and because dorsal ACC has been consistently associated with pain processing [32]. Moreover, Glutamate is the major excitatory neurotransmitter in the ACC and it is not surprising that N_2O compounds, as NMDA antagonists, modulate the activity in the ACC, which was found to participate to relief of both acute and chronic pain [33]. The opposite effect on dorsal ACC is not completely clear but it can be hypothesized that reduction in dorsal ACC connectivity relates to a significant analgesic action in healthy controls whereas non-responders may have felt the exposure as a negative or painful experience because they were disappointed they had no clinical improvement and suffering relief. Finally, while reduction in sgACC connectivity may be viewed as a marker of antidepressant response, elevation in dorsal ACC connectivity may provide, on the contrary, a marker of unsuccessful antidepressant response with EMONO.

Regarding efficacy and safety of EMONO in our study, 45% of responders could be considered the average level of antidepressant response observed in the literature with N_2O. Although the literature on N_2O antidepressant efficacy is still scarce to date, response rate range from 20–42% after a single exposure [3–5] and the relatively high rate of responders in our study may be accounted by the relatively low level of resistance of our patients (participants with only one antidepressant failure could be included) and because of the open labeled designed of the study. Tolerability was generally good, although participants experienced relatively frequent vomiting. Nausea is the most frequent side effect with N_2O compound and can affect up to 20% of the participants in the antidepressant trial, whereas vomiting is less frequent and can affect up to 10% of the participants. It must be noted that vomiting happened mostly with the first participants and largely disappeared when we suggested to the participants to not have eaten anything before EMONO exposure.

Limitations of our study include the small sample size which reduces the power of our statistics and larger studies are needed to confirm our findings. The open-label design of the trial may also constitute a

limitation since it is unknown whether changes in ACC connectivity may also occur in responders to placebo. The use of EMONO can be considered a limitation in that we cannot disentangle the specific effect of N_2O over oxygen and we cannot strictly ruled out the possibility that enriched oxygen have contributed to brain changes, especially because it has been found that repeated O2 can improve symptoms of depression [34]. However, N_2O is considered a glutamate antagonist, unlike O2, which is highly concentrated in ACC and changes in the connectivity in this brain region may be more likely due to N_2O. In addition, N_2O had more vasodilatation action compared to O2 and the very large elevation of BTP is more likely due to N_2O.

5. Conclusion

Our findings provide cerebral mechanisms for the rapid antidepressant action of N_2O, which may be considered partly similar to ketamine, with reduction in the sgACC-precuneus connectivity being associated with antidepressant response, in addition to a potential implication of elevation in CBF that may facilitate drug delivery to glutamatergic neurons. These findings are important to support the therapeutic action of N_2O compounds, which are only recently being considered antidepressants and may be considered initial findings consistent with the literature of a novel class of glutamatergic fast-acting antidepressant. In addition, our study provides potential markers of treatment response, namely the connectivity of the ACC and elevation of brain pulsations, which could be used in future larger studies and ultimately in clinical routine.

Declarations

ACKNOWLEDGEMENTS

The PROTOBRAIN study was supported by grants from “La Fondation de l’Avenir pour la Recherche Médicale (grant no. DLAM_2017251)” and from “La Fondation Planiol pour la Recherche sur le Cerveau.”

CONFLICT OF INTEREST

TD reports personal fees from Janssen and Lundbeck. WEH reports personal fees from Air Liquide, Eisai, Janssen, Lundbeck, Otsuka, UCB and Chugai. VC reports personal fees from Janssen, Bristol Myers Squibb and AA Pharma. All other authors declare no competing interests.

References

1. Guimarães MC, Guimarães TM, Hallak JE, Abrão J, Machado-de-Sousa JP. Nitrous oxide as an adjunctive therapy in major depressive disorder: a randomized controlled double-blind pilot trial. Braz J Psychiatry. 2021;43:484–493.
2. Liu H, Kerzner J, Demchenko I, Wijeysundera DN, Kennedy SH, Ladha KS, et al. Nitrous oxide for the treatment of psychiatric disorders: A systematic review of the clinical trial landscape. Acta

Psychiatrica Scandinavica. 2022;146:126–138.

3. Nagele P, Palanca BJ, Gott B, Brown F, Barnes L, Nguyen T, et al. A phase 2 trial of inhaled nitrous oxide for treatment-resistant major depression. Sci Transl Med. 2021;13.
4. Nagele P, Duma A, Kopec M, Gebara MA, Parsoei A, Walker M, et al. Nitrous oxide for treatment-resistant major depression: a proof-of-concept trial. Biol Psychiatry. 2015;78:10–18.
5. Yan D, Liu B, Wei X, Ou W, Liao M, Ji S, et al. Efficacy and safety of nitrous oxide for patients with treatment-resistant depression, a randomized controlled trial. Psychiatry Res. 2022;317:114867.
6. Quach DF, de Leon VC, Conway CR. Nitrous Oxide: an emerging novel treatment for treatment-resistant depression. J Neurol Sci. 2022;434:120092.
7. Izumi Y, Hsu F-F, Conway CR, Nagele P, Mennerick SJ, Zorumski CF. Nitrous oxide, a rapid antidepressant, has ketamine-like effects on excitatory transmission in the adult hippocampus. Biol Psychiatry. 2022;92:964–972.
8. Chamaa F, Bahmad HF, Makkawi A-K, Chalhoub RM, Al-Chaer ED, Bikhazi GB, et al. Nitrous oxide induces prominent cell proliferation in adult rat hippocampal dentate gyrus. Front Cell Neurosci. 2018;12.
9. Gerlach AR, Karim HT, Peciña M, Ajilore O, Taylor WD, Butters MA, et al. MRI predictors of pharmacotherapy response in major depressive disorder. Neuroimage Clin. 2022;36.
10. Alexander L, Jelen LA, Mehta MA, Young AH. The anterior cingulate cortex as a key locus of ketamine's antidepressant action. Neurosci Biobehav Rev. 2021;127:531–554.
11. Desmidt T, Brizard B, Dujardin P-A, Ternifi R, Réméniéras J-P, Patat F, et al. Brain Tissue Pulsatility is Increased in Mid-Life Depression: A comparative study using ultrasound tissue pulsatility imaging. Neuropsychopharmacology. 2017. 6 June 2017. https://doi.org/10.1038/npp.2017.113.
12. Desmidt T, Dujardin P-A, Brizard B, Réméniéras J-P, Gissot V, Dufour-Rainfray D, et al. Decrease in ultrasound Brain Tissue Pulsations as a potential surrogate marker of response to antidepressant. J Psychiatr Res. 2022;146:186–191.
13. Desmidt T, Gissot V, Dujardin P-A, Andersson F, Barantin L, Brizard B, et al. A case of sustained antidepressant effects and large changes in the brain with a single brief exposure to nitrous oxide. The American Journal of Geriatric Psychiatry. 2021. 4 February 2021. https://doi.org/10.1016/j.jagp.2021.01.138.
14. Dashdorj N, Corrie K, Napolitano A, Petersen E, Mahajan RP, Auer DP. Effects of subanesthetic dose of nitrous oxide on cerebral blood flow and metabolism: a multimodal magnetic resonance imaging study in healthy volunteers. Anesthesiology. 2013;118:577–586.
15. Penny WD, Friston KJ, Ashburner JT, Kiebel SJ, Nichols TE. Statistical Parametric Mapping: The Analysis of Functional Brain Images. Elsevier; 2011.
16. Patel AX, Kundu P, Rubinov M, Jones PS, Vértes PE, Ersche KD, et al. A wavelet method for modeling and despiking motion artifacts from resting-state fMRI time series. Neuroimage. 2014;95:287–304.

17. Behzadi Y, Restom K, Liau J, Liu TT. A component based noise correction method (CompCor) for BOLD and perfusion based fMRI. NeuroImage. 2007;37:90–101.
18. Lindquist MA, Geuter S, Wager TD, Caffo BS. Modular preprocessing pipelines can reintroduce artifacts into fMRI data. Hum Brain Mapp. 2019;40:2358–2376.
19. Rolls ET, Huang C-C, Lin C-P, Feng J, Joliot M. Automated anatomical labelling atlas 3. Neuroimage. 2020;206:116189.
20. Desmidt T, Andersson F, Brizard B, Dujardin P-A, Cottier J-P, Patat F, et al. Ultrasound Measures of Brain Pulsatility Correlate with Subcortical Brain Volumes in Healthy Young Adults. Ultrasound Med Biol. 2018;44:2307–2313.
21. Siragusa MA, Brizard B, Dujardin P-A, Réméniéras J-P, Patat F, Gissot V, et al. When classical music relaxes the brain: An experimental study using Ultrasound Brain Tissue Pulsatility Imaging. Int J Psychophysiol. 2020;150:29–36.
22. Evans DH. Colour flow and motion imaging. Proceedings of the Institution of Mechanical Engineers, Part H: Journal of Engineering in Medicine. 2009. 9 July 2009. https://doi.org/10.1243/09544119JEIM599.
23. Yiu BYS, Lai SSM, Yu ACH. Vector projectile imaging: time-resolved dynamic visualization of complex flow patterns. Ultrasound Med Biol. 2014;40:2295–2309.
24. Ternifi R, Cazals X, Desmidt T, Andersson F, Camus V, Cottier J-P, et al. Ultrasound measurements of brain tissue pulsatility correlate with the volume of MRI white-matter hyperintensity. J Cereb Blood Flow Metab. 2014;34:942–944.
25. Nonparametric permutation tests for functional neuroimaging: A primer with examples. https://doi.org/10.1002/hbm.1058.
26. Demchenko I, Tassone VK, Kennedy SH, Dunlop K, Bhat V. Intrinsic Connectivity Networks of Glutamate-Mediated Antidepressant Response: A Neuroimaging Review. Front Psychiatry. 2022;13.
27. Hamilton JP, Farmer M, Fogelman P, Gotlib IH. Depressive Rumination, the Default-Mode Network, and the Dark Matter of Clinical Neuroscience. Biol Psychiatry. 2015;78:224–230.
28. Kucewicz JC, Dunmire B, Giardino ND, Leotta DF, Paun M, Dager SR, et al. Tissue Pulsatility Imaging of Cerebral Vasoreactivity During Hyperventilation. Ultrasound in Medicine & Biology. 2008;34:1200–1208.
29. Kucewicz JC, Dunmire B, Leotta DF, Panagiotides H, Paun M, Beach KW. Functional Tissue Pulsatility Imaging of the Brain During Visual Stimulation. Ultrasound in Medicine & Biology. 2007;33:681–690.
30. Lin Y, Pan Y, Wang M, Huang X, Yin Y, Wang Y, et al. Blood-brain barrier permeability is positively correlated with cerebral microvascular perfusion in the early fluid percussion-injured brain of the rat. Lab Invest. 2012;92:1623–1634.
31. Zhang X, Zhu HC, Yang D, Zhang FC, Mane R, Sun SJ, et al. Association between cerebral blood flow changes and blood-brain barrier compromise in spontaneous intracerebral haemorrhage. Clin Radiol. 2022;77:833–839.

32. Lieberman MD, Eisenberger NI. The dorsal anterior cingulate cortex is selective for pain: Results from large-scale reverse inference. Proc Natl Acad Sci U S A. 2015;112:15250–15255.
33. Bliss TVP, Collingridge GL, Kaang B-K, Zhuo M. Synaptic plasticity in the anterior cingulate cortex in acute and chronic pain. Nat Rev Neurosci. 2016;17:485–496.
34. Bloch Y, Belmaker RH, Shvartzman P, Romem P, Bolotin A, Bersudsky Y, et al. Normobaric oxygen treatment for mild-to-moderate depression: a randomized, double-blind, proof-of-concept trial. Sci Rep. 2021;11:18911.

Figures

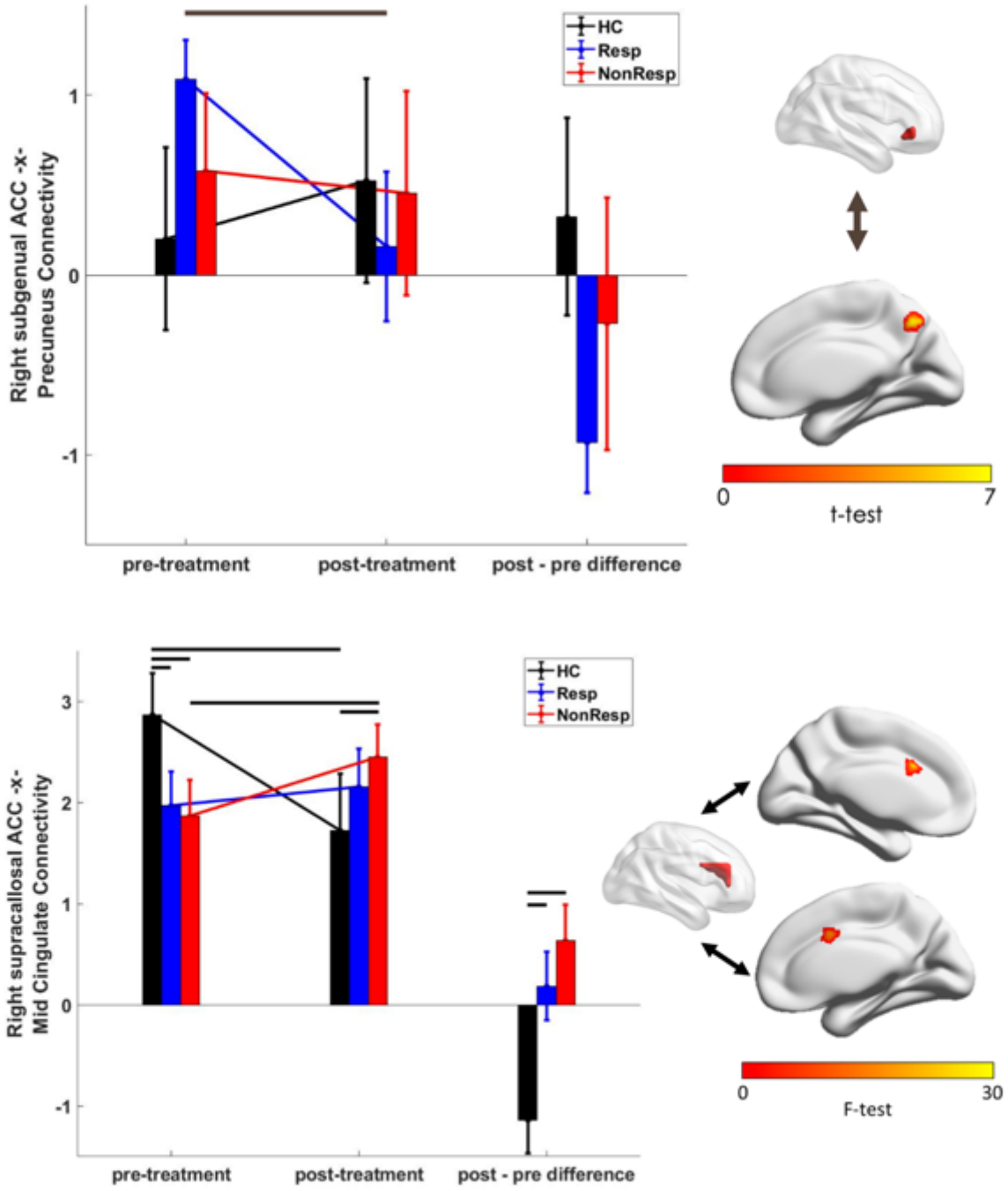

Figure 1

Voxel-wise results and plots. Right sgACC-precuneus connectivity significantly declined in non-responders but did not change in other groups. Right supracallosal ACC-mid cingulate connectivity showed group x time interactions, where HC and non-responders showed decreased and increased, respectively, connectivity while responders showed no change in connectivity from pre- to post-treatment. HC had significantly greater connectivity than responders and non-responders pre-treatment, but there were no

differences post-treatment between HC and responders while non-responders had significantly greater connectivity post-treatment.

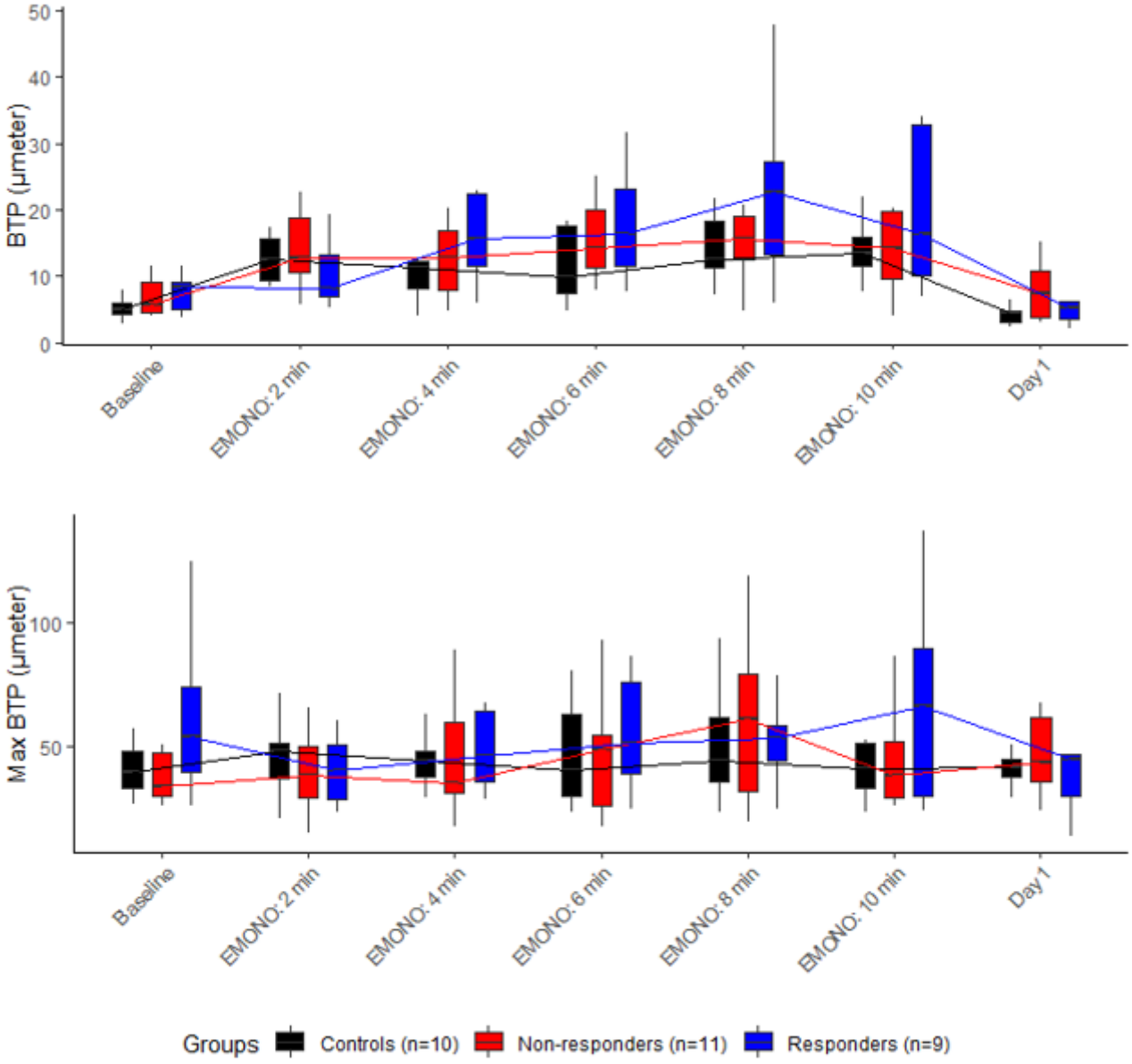

Figure 2

Changes in MeanBTP (upper graph) and in MaxBTP (lower graph) between pre-exposure (baseline), per-exposure and post-exposure (24H post N_2O) among responders (blue, n=9), non-responders (red, n=11) and healthy controls (green, n=10). MeanBTP significantly increased in all the groups between pre- and per-exposure, whereas there were no significant changes between pre- and post-exposure in any group. MeanBTP significantly increased per-exposure but only in responders and not in non-responders or healthy controls. We observed no significant changes in MaxBTP.

Supplementary Files

This is a list of supplementary files associated with this preprint. Click to download.

- 2023JanSupplementaryMaterial11.docx